

REMARKS

Applicants submit herewith amended claims, a substitute specification and proposed corrections to drawings in response to the Examiner's Office Action dated May 14, 2003. In that Action the Examiner objected to the application and rejected the claims on several grounds. These objections and rejections are treated seriatim below in the order that the Examiner raised them.

Drawings. The Examiner objected to the drawings for their use of reference characters in referring to disparate structure, for the appearance of three characters (49, 50, 53) which are not discussed in the specification, and for failure to label FIGURES 9A and 9B as "prior art". In response, Applicants submit herewith a new set of drawings, with one copy (Attachment D) being marked up in red, to show proposed corrections. Many new characters have been used so that no one character will identify unrelated parts. Characters (49, 50, 53) have been removed. FIGURES 9A and 9B have been labeled -- prior art --.

In addition, the Applicants have discovered that the last set of drawings contain certain errors in representing the structure. The new set of drawings corrects these. Specifically, in Fig. 1 the right-facing face of the cube has been shaded, so as to comport with the detailed description of this Figure, found in the Background of the Invention p. 2, lines 13 – 15 of the original specification. Figure 9B has been changed to show that layers 1 and 2, which were made in the process step shown in Figure 9A, have layer 4 added to them at the point in the

process shown in Figure 9A. Layers 1 and 2 together comprise layer 3. Support for this change can be found in the original specification at p. 17, lines 16 – 20.

Figure 14 has been revised to show that common contact 23 adjoins conductive interconnect 28 and extends through layers 20 and 21. Common contact 23 also does not invade HgCdTe layer 8 to the original extent shown. Support for these changes can be found Figs. 15I – L as initially filed and by the original detailed description e.g. at p. 32, lines 1 –2.

Figure 15K has been revised to show that the metal interconnects contact the (p) regions 14 and 15, a structure shown in Figure 14 as initially presented. Fig. 15L shows common contact 23 and its interconnect as separate structure, seen for example in Fig. 13 as initially presented.

Applicants do not intend to add any new matter with these drawing changes, but believe that the drawings will be more correct and internally consistent with their entry.

Specification. The Examiner objected to the specification because a related application was incorporated by reference, and because of two other informalities. In response, Applicants submit a substitute specification, in marked up form and in clean form. The related application is more particularly identified but is no longer incorporated by reference. The informalities noted by the Examiner have been corrected. Applicants have also made numerous changes to the recitation of reference characters to comport with the new

drawings. Applicants have also corrected various grammatical errors. Applicants have added no new matter by these changes.

Claim Objections. The Examiner noted various informalities in Claims 4, 5, 8, 12 and 13. In the amendments Applicants have made appropriate corrections.

Claim Rejections – 35 USC 112. The Examiner rejected Claim 13 under 35 USC 112, first paragraph because, in the Examiner's view, the claim's recited step of etching the Si wafer with a concentrated solution of ammonium fluoride (NH₄F) solution is not supported in the specification with sufficient detail that a person of ordinary skill in the art could practice the claimed invention. Applicants respectfully traverse this ground for rejection.

As the Examiner admits, the specification discloses (p. 21, lines 4 – 11) that concentrated NH₄F (20% - 40%) is used. Claim 13 as originally presented (which therefore is a portion of the original specification) adds that this is a *solution*. The original specification also tells us that this is a second "wet etch" (line 14), and that the time of etching preferably is 30 +/- 10 seconds, as longer periods than this produces rough surfaces with [111] facets (lines 13- 14). The Examiner states that there is no disclosure of the composition of the concentrated NH₄F etchant nor of the temperature during which the etch is performed, and that despite the rest of the detail given, a person of ordinary skill in this art would not have enough information to make and use the invention.

As it happens, the balance of the NH_4F solution is *water*, and the temperature at which the etch is conducted is *room temperature* – prior to the introduction of the wafer into the MBE reactor. Given that NH_4F is polar, water would be the first choice in polar solvents. In the absence of phrases such as “hot etch” or “as buffered with HF”, the skilled artisan would automatically assume that the NH_4F solution was an aqueous one, and that the etch was to be carried out at room temperature. Kaganowicz et al. U.S. Patent No. 4,705,760, at Col. 2, lines 59 – 68 through Col. 3, lines 1 – 6, cited by the Examiner, recites these very details on composition and etch conditions, at least with respect to etching indium phosphide: using as one of the ingredients a 40% aqueous solution of ammonium fluoride, and carrying out the etch at room temperature. Ammonium fluoride is commonly available in 40% aqueous solution (see product safety sheet, Attachment E). It is not an exotic chemical in this art, but is well-known, as is shown by Kaganowicz and e.g. Semiconductor Fabtech (8th Ed. May, 1997) pp. 135 – 138 (Exhibit F). Once a person of ordinary skill understood that a low-temperature passivation and cleaning of an elemental silicon surface could be had by dihydride (as opposed to the more conventional oxide) termination, and that dihydride termination could in turn be created by dipping the wafer in a 20% - 40% concentrated NH_4F solution, he or she could practice this etch step right away without any further information. Applicants therefore request the Examiner to withdraw this ground for rejection.

The Examiner has rejected Claim 5 under 35 USC 112, second paragraph, as being incomplete for omitting essential structural cooperative relationships, particularly commenting on the occurrence of “a horizontal plane.” Per the Examiner’s suggestion, this has been replaced with the “face” of the silicon layer.

The Examiner rejected Claim 13 as being indefinite for its recitation, without antecedent basis, of "Si wafer" and "the passivation layer." Applicants' amendment corrects these informalities, as well as similar informalities noted in Claim 14. Applicant has also amended Claims 2, 4, 6, 9, 11 and 14 to correct other discovered problems with antecedent basis.

Claim Rejections under 35 USC 103. Substantively, the Examiner first rejects claims 1, 3, 6, 10 and 11 as allegedly obvious in view of a four-way combination of Bevan et al. US Patent No. 5,838,053; Tew et al., U.S. Patent No. 4,686,373; Zanio et al., U.S. Patent No. 4,910,154; and Goodwin, U.S. Patent No. 5,300,777. Applicant respectfully traverses these grounds for rejection, as none of these references, alone or in permissible combination, teaches or suggests an infrared sensing device (1) built on an elemental silicon, (2) wherein this elemental silicon already incorporates a readout integrated circuit (ROIC) at its face, (3) wherein an infrared detecting cell is formed in a mesa of II-VI semiconductor material, and (4) wherein this mesa is epitaxially grown on the face of the ROIC-containing silicon layer.

Most of the Bevan et al. reference concerns itself with the prior art hybrid technology, in which no attempt is made to fabricate an ROIC in that substrate which (indirectly) supports the HgCdTe detector element. Instead, as is best shown in Bevan et al.'s Figure 5, indium bumps 24, 26 are used to mate a silicon ROIC 20 to the rest of the structure 22. Most of the disclosure concerns this old solution, the drawbacks of which are discussed in Applicants' own background. But Figure 6 and a single paragraph at Col. 5, lines 40 – 48, describe an

alternative embodiment. Bevan et al. say that the photodiode 30 (created by layers 14a-c, 16, 18a-b) is coupled to the "processing circuitry" 20 via a contact 32 disposed in a via.

What Bevan et al. do not do is tell the skilled person in this art how this briefly described device might be constructed. Column 2, lines 40 – 47 describe a 950° C oxide desorption step that would effectively destroy any ROICs which had been fabricated in the silicon substrate. Attempting to implement ROICs *after* the creation of the relatively heat-labile layers 14a-c, 16, 18a-b would likewise not result in an operational device. In sum, Bevan et al.'s off-hand, brief description of this via-interconnected device does not contain enough information for a person of ordinary skill to make it. Bevan et al. also do not disclose or suggest a mesa (Claim 1), adjacent layers of II-VI material having different bandgaps (Claim 3), a single buffer layer of II-VI material epitaxially grown on the face of the elemental silicon layer, which in turn has HgCdTe epitaxially grown on it (Claim 6; Bevan et al. instead resort to four successive buffer layers having progressively changing lattice constants), or at least two detecting cells formed in the same mesa (Claim 11). Relative to Claim 11, it is noted that Bevan et al.'s Figure 6 is a cross-sectional view of a *via* around the walls of which a *single* detector element has been fashioned. There is no disclosure or suggestion of how multiple detector cells might be segregated one from the other in this structure.

The Examiner takes repeated note of the fact that Bevan et al. incorporated by reference the Goodwin patent. Applicants take note of what the Goodwin patent was incorporated by reference *for*: another hybrid array in which the silicon ROIC processor chip

is joined, via indium bumps, to HgCdTe photodiodes formed on a separate insulator substrate. If *arguendo* Goodwin's (n) HgCdTe regions are considered mesas, they are *not* "mesas" which have been grown on a silicon layer, much one less one on which a readout integrated circuit has already been formed. Further, Claim 1 requires that the detecting cell be formed *in the mesa*, not just half of it. Claims 10 and 11 recite two II-VI layers, both of which are contained in the mesa, rather than just one of them.

The Examiner also states that Tew et al. and Zanio et al. disclose mesas. But neither discloses or suggests an operational detector device formed in a II-VI mesa epitaxially grown on a face of an elemental silicon layer, where that silicon layer has had an ROIC fabricated at the face. Tew et al. avoid the difficulties of fabricating this sort of structure by *gluing* the HgCdTe "mesa" onto the silicon processor; see Fig. 1, epoxy layer 60. The non-monolithic nature of this structure makes it inapposite to the claimed invention, and there is therefore no suggestion to combine any of its structure with the other references.

Zanio et al. show a mesa – but only as a structure to be avoided:

To begin with, it is not possible to directly grow detector quality HgCdTe on the surface of the silicon wafer. An additional problem is the interconnection of the elevated detector arrays with the silicon circuitry. Because the metallic interconnections are vapor deposited in a direction nearly normal to the wafer surface, the steep sides of the detector arrays result in poor metallic step coverage and poor interconnections.

Zanio et al., Col. 1, lines 32 – 39. To overcome these problems, Zanio et al. go in directions other than those taught and claimed by the present invention. First, to overcome the problem of growing HgCdTe on silicon substrates, instead of using a tilted Si substrate and a II-VI buffer layer (see Claims 1, 3, 10 and 11), Zanio et al. use a buffer layer of gallium arsenide (a III-V material). Second, instead of using a mesa with sloped sides to improve conductive interconnect step coverage (as is recited in Claims 6 and 11), they abandon mesas altogether, instead sinking their detector cell into a recess 30 (Figure 3). Because of these different approaches, there is no suggestion to combine the teachings of Zanio et al. with other references describing cells featuring mesas (and *a fortiori*, glued-on ones), cells employing a tilted Si substrate, or cells avoiding the use of a III-V buffer layer.

The Examiner rejects claims 2 and 4 as allegedly obvious in view of a patching-together of five references: Bevan et al., Tew et al., Zanio et al., Goodwin and Chapman et al., U.S. Patent No. 5,581,084. Chapman et al. teach a common anode contact, but otherwise merely show the prior art: a non-Si substrate (CdZnTe, Col. 5 line 15), no readout integrated circuit formed in the substrate, and hence no contact to a common of such an ROIC. Instead, Chapman et al. connect either to indium bumps 24, 28 (Figs. 4 – 5) or to a bus 30, 32 which connects to an indium bump (not shown) at a peripheral region of the array (Col. 5, line 66 – Col. 6, line 12). Chapman does not show an interconnect of any kind from a II-VI mesa to an ROIC formed at the face of a silicon layer on which the mesa had been epitaxially grown, and not even an impermissible patching of it and the other four references discloses or suggests the claimed invention.

The Examiner rejects claim 5 in view of a five-way combination of Bevan et al., Tew et al., Zanio et al., Goodwin and Bean et al., U.S. Patent No. 3,936,929. Bean et al. show a mesa 8 of elemental silicon on a polysilicon substrate. The mesa 8 is created by lapping, etching or otherwise from a silicon substrate 2 (Col. 3, lines 32 – 34). Sidewalls at an angle of 46 or 54 degrees may be created by “orientation-dependent etching” (Col. 4, lines 13 – 16). Applicants nonetheless do not understand how this reference, which does not deal with II-VI compound semiconductors at all or etch chemistries suitable for such compound semiconductors, makes 40 to 50 degree sloped sides on a II-VI mesa obvious – there is certainly nothing in Bean et al. which tells the reader how to arrive at this result. The Examiner should withdraw his application of the inapposite Bean et al. reference to this invention and the ground for rejection based thereon likewise should be withdrawn.

The Examiner next rejects Claims 7 – 9 as allegedly obvious in view of a five-way combination of Bevan et al., Tew et al., Zanio et al., Goodwin and Koehler, U.S. Patent No. 4,137,544. The Examiner cites to Koehler to show first and second layers of (n) HgCdTe and a (p) region created by arsenic implantation. What Koehler does *not* show or suggest are two layers of HgCdTe having different bandgaps, as are required by all of these claims; Koehler’s layers differ from each other only in dopant concentration. Koehler is otherwise irrelevant: it does not show mesas of HgCdTe, or their epitaxial growth on silicon, or the employment of II-VI buffer layers, or the tilting of an Si substrate, or the pre-fabrication of an ROIC on the silicon layer used to grow the HgCdTe structures. Claims 7 – 9 are patentable in view of this cited combination and of the rest of the prior art.

The Examiner rejects independent method Claim 12 in view of Bevan et al., Goodwin, de Lyon, U.S. Patent No. 5,306,386 and Wu et al., U.S. Patent No. 6,043,141. Claim 12 includes the steps of etching an exposed Si [001] surface to yield a dihydride terminated smooth [001] surface, and, after inserting the thus-passivated wafer into an MBE chamber, thermally cleaning the dihydride terminated surface at a temperature of less than 500° C. Thereafter, the II-VI semiconductor material is epitaxially grown on the thermally cleaned silicon, at a temperature of less than 500° C. so as not to degrade the ROIC circuitry already in the wafer.

Wu et al. and de Lyon don't show anything like this. Applicants are unable to discern any passivation step in Wu et al. at all; the reference concentrates on what happens once a II-VI wafer is inside the MBE chamber. Use of a Si substrate is nowhere disclosed in the reference. De Lyon show passivation with *arsenic*, not hydrogen. De Lyon's monoatomic layer of arsenic persists during the process; in contrast, the Applicants' dihydride passivation layer is removed by a low-temperature thermal cleaning once the wafer has been inserted into the MBE chamber. None of the remaining references shows or suggests these claimed limitations.

Finally, in rejecting dependent Claims 13 – 15, the Examiner apparently has been forced to base his rejection on an improbable combination of *eleven* references, a number large enough to suggest, by itself, the nonobviousness of the claimed invention. These references include the four distinguished above and La Chapelle, Jr. (U.S. Patent No. 5,366,934), McConnell et al. (U.S. Patent No. 4,776,532), Hetrick et al. (U.S. Patent No.

6,096,149), Kaganowicz et al. (U.S. Patent No. 4,705,760), Norimatsu et al. (U.S. Patent No. 6,049,638), Tew et al., and Koehler.

LaChapelle, Jr. teaches passivation using *sulfide*, not dihydride. It does not concern itself with preparation of silicon surfaces for epitaxially growing mesas of II-VI detector elements.

McConnell et al. concerns itself mostly with the mechanical aspects of a system for treating wafers with process fluids. At Col. 23, lines 24 – 54, the inventors go through various possibilities for employing their wet-etch system, coming closest to the claimed invention in disclosing that HF or $\text{NH}_4\text{F} + \text{HF}$ (note that the concentrations and temperatures are missing) can be used to etch silicon dioxide. McConnell nowhere suggests passivation of any sort, much less a dihydride passivation or its subsequent in situ low-temperature removal.

Hetrick et al. passivate (actually, permanently coat) parts using amorphous hydrogenated carbon (AHC), a particularly bad choice for the purposes of the invention. The invention provides a temporary passivation layer which can be thermally removed at a low temperature (no greater than 500°C) in the MBE chamber. AHC creates carbides which will desorb only at temperatures of about 1000°C , a temperature which would destroy or seriously degrade the ROIC formed on the silicon wafer. It is not surprising that Hetrick does not discuss II-VI semiconductor processing or the union of II-VI semiconductor elements with Si support surfaces.

Kaganowicz et al. disclose steps for processing workpieces leading to indium phosphide (Group III-V) photodetectors. The reference discusses the passivation of

InGaAs/InP semiconductor bodies with silicon oxynitride. NH_4F is used only in a cleaning phase prior to passivation, and does not yield a dihydride terminated surface, such as one which the invention provides to temporarily passivate a site next used for the growth of a II-VI compound semiconductor structure. The reference does not concern itself with a passivation layer which can be later removed in a low-temperature step.

Norimatsu et al. disclose techniques for fashioning sloped optical surfaces in indium phosphide and silicon, creating 54.7 degree angled surfaces. The reference nowhere discloses wet etch techniques as applied to Group II-VI materials, whether by Br/HBr solutions or otherwise.

That Tew et al. and Koehler teach photoresist masks do not make up for the claimed process steps not found anywhere in this collection of art, namely the use of a dihydride terminated passivation layer which can be removed from an elemental silicon site in an MBE chamber, at a relatively low temperature, prior to the epitaxial growth of a II-VI semiconductor structure.


Applicants have submitted a new independent method claim 16. It is patentable at least for the reasons given for claim 12: the prior art does not disclose or suggest passivating a site on a face of a silicon layer with dihydride terminations, removing thus passivation in a low temperature step in situ, and then epitaxially growing a Group II-VI compound semiconductor structure on the site.

In sum, none of these cited references, taken alone or in combination, fairly teaches or suggests the claimed infrared detector device or the recited method of making it. Having

overcome the Examiner's other rejections and objections, Applicants respectfully request the Examiner to issue a notice of allowance on the claims as amended.

A fee is due because of the addition of an independent claim. A fee calculation sheet is included. The Director is hereby authorized to charge any deficiency or credit any overpayment to Deposit Account No. 18-2284 of Piper Rudnick, duplicate copy attached.

Respectfully submitted,



Jefferson Perkins
Reg. No. 31,407

PIPER RUDNICK
P.O. Box 64807
Chicago, IL 60664-0807
(312) 368-7073



Attachment A
Marked-up Copy of Substitute Specification

MONOLITHIC INFRARED FOCAL PLANE ARRAY DETECTORS

RELATED APPLICATION:

The present application is related to ~~and fully incorporates by reference to~~
U.S. Patent Application Serial No. 09/834,446, filed April 13, 2001 ~~MMMM, DD,~~
~~2001, Entitled “~~ , entitled “MULTISPECTRAL MONOLITHIC INFRARED FOCAL
PLANE ARRAY DETECTORS”.

FIELD OF THE INVENTION

The present invention relates to infrared sensing ~~device~~devices, and more specifically
monolithic infrared imaging arrays based on the direct growth of infrared sensitive mercury
5 cadmium telluride material structure on custom-fabricated read-out electronics on specially
oriented silicon substrates.

BACKGROUND OF THE INVENTION

Semiconductors are either naturally occurring or artificially synthesized materials in
which the atomic arrangement gives rise to a specific atomic potential that forbids electrical
10 ~~carriers~~carriers (electrons or positive charges, known as holes) to freely move and therefore carry
electrical currents. They act as insulators for as long as there is no additional energy provided to
excite these carriers across the forbidden gap (called a band gap) that is generated by the atomic
potential. An electrical current can be obtained by the excitation of electrons across the forbidden
band. The necessary ~~Necessary~~ energy can be generated in different ways and of interest for

radiation detection is the energy carried by the electromagnetic radiation waves. ~~The incoming radiation has to be~~ This periodicity Periodicity in the atomic arrangement is of utmost importance for the electrical behavior of the crystal. A polycrystalline material has a short-range order, a specific geometrical positioning of the atoms in a lattice, but lacks long-range order.

- 5 Only by performing a combination of translations and rotations one can recover the same geometrical arrangement of an initial test region.

~~The p~~Polycrystalline material is formed by a multitude of grains consisting of individual single crystals. A long-range order means that by translating the crystal in any direction one recovers exactly the same structural arrangement of the atoms. A unit cell can be therefore
10 defined, and the entire crystal can be regained by translations of this unit cell. An amorphous material lacks both short and long-range order, and consequently lacks any periodicity in its atomic arrangement.

FIG. 1 shows the unit cell for a cubic crystalline lattice and several crystal directions. The crystal planes are planes that contain atoms and are perpendicular to the respective direction. The
15 (100) plane in a cubic lattice is shown as shaded in FIG.1. Obviously, in the case of a cubic unit cell the chosen orientation of the reference system is arbitrary, thus the (100), (010) and (001) planes are equivalent. All the equivalent planes form a family of planes and are called by a generic name, which is one of the family member names. The atoms can occupy positions on the nodes of the grid or at intersections of principal lines within the unit cell (such as the center of
20 lateral cubic faces or the intersection of body diagonals of the cube). The atoms can, as well, occupy positions at certain coordinates around the nodes or intersections of principal lines in what is called a basis. A cubic unit cell with atoms sitting at the nodal position as well as in the center of each cubic face is called a face centered cubic (fcc). Mercury cadmium telluride

(HgCdTe or MCT) is an fcc lattice with a basis in which a secondary set of atoms is situated at $\frac{1}{4}$ of the cubic length away from the fcc atoms in the (111) direction.

Mercury cadmium telluride is a semiconductor widely used as an infrared detector material. It consists of elements positioned in group II (Hg, Cd) in the periodic table of elements and in group VI (Te). The crystalline MCT is formed as a ternary material from an HgTe (mercury telluride) crystal lattice in which a certain percentage of Hg atoms is being replaced by Cd atoms.

By varying the amounts of Cd atoms in replacement of Hg atoms, the electrical properties of the entire crystal can be tailored to suit the absorption and subsequent conversion of the incident infrared radiation into electrical current. Thus, short wavelength infrared (SWIR) MCT has a Cd percentage that allows radiation absorption of short wavelengths. Similarly, mid-wavelength (MWIR) MCT has a Cd percentage that allows radiation absorption of medium wavelengths, and long wavelength (LWIR) MCT has a Cd percentage that allows radiation absorption of long wavelengths.

The flexibility of matching the electrical behavior of the crystal to certain application requirements by adjusting the composition of the crystal is known as band gap engineering, and is one of the great advantages of MCT. Several techniques are available for producing MCT and by far, MBE molecular beam epitaxy is the most reliable.

Molecular beam epitaxy (MBE) is a chemical vapor deposition (CVD) method in which the crystal is grown on a template (substrate) from atomic and/or molecular fluxes obtained by thermal evaporation of the charge material. The growth process occurs in an ultra-high vacuum (UHV) environment to minimize the presence of foreign atoms. Polycrystalline and/or amorphous material are loaded into crucibles and constitute the charge. During the growth, the

substrate is kept at predefined temperatures to ensure that sufficient energy is transferred to the surface to achieve specific reactions. The fluxes are adjusted by the temperatures at which the charge materials are kept. In this way the incoming atoms/molecules from the charges have to spend a certain residence time on the surface while traveling/diffusing around in order to find a geometrical position that minimizes the surface energy.

In order to control and to enhance or modify the electrical properties of the materials grown by MBE one can use this method to add certain impurities (dopants) to the primary material. This added control offers a large advantage since it reduces the post growth processing along with the costs and increases the yield factor.

The substrate is of paramount importance for the MBE growth of crystalline materials. Its choice is primarily dictated by the lattice parameters that have to closely match the ones of the intended new material. Exceptions are rare and mismatches create unwanted density of defects/dislocations.

In order to act as a template, the substrate itself should be a single crystal and one has to expose the periodic arrangement of the bulk material. Typically, the bonds between atoms are saturated (i.e. an atom/ion uses all of its available electrons for bond formation with its neighboring atoms). At the surface, the lack of periodicity in the direction perpendicular to the plane forces the atoms lying on the surface to react (use their available electrons) and bond with other elements, different than those present in the bulk of the material. These elements that are present at the surface are called contaminants. Such a surface is useless for the MBE growth of single crystalline materials.

For the growth of MCT one can use as substrate bulk cadmium zinc telluride (CdZnTe) for which lattice matching occurs at a Zn percentage close to 4%. A constant demand for larger

area detectors prevents the use of CdZnTe as substrates since they are available in limited sizes only. Bulk CdZnTe is also expensive and brittle reducing further its use in production environments. When using CdZnTe as substrate one is limited by the current device fabrication technology.

5 The crystals used as substrates (Silicon, CdZnTe and others) are fabricated by cooling a melt of material (pure elements or compounds) in a way that allows crystal formation. Once crystallized, the previously formed ingot is cut into wafers with various orientations. Since the wafer is a single crystal (hence it contains a large number of unit cells, to be viewed as "bricks") its surface can have various morphologies. The surface orientation of the substrate is very
10 important since the initial nucleation process takes place on it. At this interface between the new crystal and the substrate the defects can be easily generated and they will further propagate through the entire crystal.

 A major problem when growing a new crystal is twin formation. Crystal seeds that nucleate at different moments in time and at different locations are uncorrelated. For various
15 surface orientations this correlation/uncorrelation can be beneficial (increasing the probability that only one crystalline orientation will survive throughout the growth process, generating a single crystal) or detrimental (supporting equally various orientations and ending with a polycrystalline material).

 A silicon surface that has orientation (001) is almost flat (FIG. 3). Theoretically, it should
20 be flat since integers of unit cells can be fit within the crystal. Other reasons are called upon to explain the surface morphology in this case. The surface energy is minimized by forming terraces. The terrace steps are always ± 1 monolayer from what is called the substrate surface. All the orientations that do not fit an integer number of the unit cell at the surface are bound to

form steps, their number increasing with the wafer area. FIG. 2 shows a schematic of a (211) surface.

Mercury cadmium telluride is by far the most sensitive and commonly used material for infrared detectors. Such detectors generate a signal whose magnitude is proportional to the intensity of the incident radiation.

Every object usually has a distribution of 'hot' and 'cold' regions in it. The image generated by an array of photon detectors consists of white and black contrast corresponding to the hot and cold regions of the object or scene. An infrared imaging device consists of a plurality of photovoltaic diodes (detectors) fabricated on an infrared sensitive material (such as HgCdTe).

When used for imaging, the signal generated by each diode has to be collected separately and multiplexed to re-construct an image on the video screen. The photovoltaic detector essentially consists of a junction formed by two dissimilar (p-type and n-type) conductivity regions in the infrared sensitive material as shown in FIGs. 5a 5A and 5b 5B. The incident infrared radiation creates electron and hole pairs, which are collected by the potential difference at the p-n junction leading to the 'signal'. ~~Also shown~~ Shown in ~~the figure~~ FIG. 5B is the energy band diagram corresponding to the p-n junction formed in a heterostructure. The heterostructure means that the band gaps of the two regions (p and n) are different. The narrow band gap side of the junction is the absorber layer whose band gap is tuned to detect the particular wavelength of interest. The band gap of the top layer (p-layer in ~~the~~ FIG. 5b 5B) is more than that of the n-layer. Such p-n junctions formed in a heterostructure reduce the surface-passivation related leakage currents.

Conventionally, the multiplexing electronics used for infrared detectors ~~is~~are fabricated separately on a silicon substrate. Indium metal bumps are then formed on each diode and the plurality of devices on the two different materials is then connected together by a 'hybridization'

process. These devices operate usually at 77K, the liquid nitrogen temperature, because one way of exciting electrons across the gap is by thermal excitation. This thermal excitation process becomes concurrent to the radiation-induced excitations. In order to reduce it and to reduce its effects (dark current, noise) the detector operates at low temperature. When cooled to this
5 temperature, the two different materials that together form the infrared imaging device (HgCdTe diode and the read-out circuit) expand at different rates. The different coefficients of expansion lead to failure of the indium bump interconnection between the infrared detector and the signal processor, resulting in poor image resolution.

Recently, a monolithic infrared imaging device to solve the problems associated with
10 hybrid type device has been proposed (Japanese Published Patent Application No. Sho. 63-46765), followed by variants of this method (U.S. Patent No. 5,410,168 and Japanese Patent Application No. Hei. 2-272766) to improve sensitivity and charge collection efficiency. We denote these methods respectively as method-A, method-B and method-C hereinafter.

The cross-sectional view of Method-A is shown in FIG. 16. A first HgCdTe narrow band
15 gap layer 32 and a second HgCdTe wider band gap layer 33 are deposited on ~~the an~~ HgCdTe substrate 31. A photodiode 34 is formed by ion implantation or the like in the first HgCdTe layer 32 by partially removing the second HgCdTe layer 33. A signal charge injection layer 42 is formed in the second HgCdTe layer 33 by ion implantation or the like. A charge transfer gate 43, a charge storage gate 44 and a CCD 45 are disposed on the second HgCdTe layer 33, and are
20 spaced apart therefrom by an insulating film 40.

The surface leakage current in this method is suppressed since both the ends of the p-n junction of the photodiode 34 are covered with wider band gap HgCdTe layer 33. However, the numerical aperture of the infrared detector is reduced since the metal interconnect 41 covers part

of the infrared absorbing ~~window~~photodiode 34. Also, the step coverage of the metal interconnect 41 is likely to fail since the two contact regions 34 and 42 are located in different planes.

FIG. 17 is a cross-sectional view of the monolithic device described in Method-B. A first
5 p-HgCdTe narrow band gap layer 33170 is buried between the semiconductor substrate 31 and a wider band gap p-HgCdTe layer 32171. A photodiode 34 is formed in the first HgCdTe layer 32171, and a source diode 38 and a drain diode 37 are formed in the second HgCdTe layer 33170 by ion implantation. An electrode 35 connects the photodiode 34 and the drain diode 37. A gate electrode 36 connects the source diode 38 with the drain diode 37. Gate 36, source 38 and drain
10 37 form a Metal Insulator Semiconductor (MIS) switch 40172 which electrical connections are made through an insulator layer 39. In this method, though the ends of the p-n junction 34 are covered with wider band gap HgCdTe layer 33170, the infrared receiving top surface involves passivation of the narrow band gap HgCdTe. This increases the surface recombination velocity, resulting in higher leakage currents. Furthermore, the signal carriers can diffuse back into the
15 light receiving region and recombine resulting in the loss of signal.

FIG. 18 is a cross-sectional view of a device according to Method-C. A wider band gap p-type HgCdTe layer 33180 of 1 to 2 microns thickness is disposed on a narrow band gap p-type HgCdTe infrared absorber layer 32181 having a thickness of about 10 microns. An n-type light receiving region 34182 and a high dopant impurity concentration n-type region 47 are formed by
20 ion implantation. A post implant annealing reduces the n-type carrier concentration in region 34182 to the order of 10^{15} cm^{-3} and extends this region into p-type substrate 32 181. In this structure, the surface of the light receiving region, both ends of the p-n junctions are disposed in the semiconductor layer with larger band gap 32181, thus reducing the recombination of charge

carriers at the light receiving region leading to lower leakage currents. However, this method involves fabrication of two back-to-back p-n junctions 47, 48 for the two contacts (p and n) for each detector and relies on the MIS device ~~26~~183 fabricated on HgCdTe to collect the photo-generated carriers. It is known that an MIS device formed on HgCdTe is noisier than that one
5 formed on silicon. This, along with the additional junction 48, is likely to increase noise current and thereby reduce the efficiency of the infrared device. Furthermore, the top regions 51 of the detectors involve passivation of narrow band gap HgCdTe material and hence do not solve the objective of p-n junctions buried in wider band gap HgCdTe material ~~33~~180.

Furthermore, in both Methods A and B, the photo-generated carriers in the vicinity of the
10 p-n junction are likely to reach the infrared receiving surface and recombine resulting in loss of signal, thereby decreasing the sensitivity of the device. This is true for region 51 in Method C too. Furthermore, in all the three Methods A to C, the signal processing circuits ~~37 to 39~~ are formed in HgCdTe instead of silicon. The density and performance of the state-of-the-art integrated circuits (IC) involving millions of transistors formed on a silicon substrate are much higher than
15 that on a HgCdTe substrate and the silicon IC technology is far more advanced and reliable.

The increased demands on the performance of silicon semiconductor devices and microcircuits have required the development of improved processing techniques. The current invention ~~is to produce~~produces high efficiency monolithic infrared devices by integrating advancements in silicon-based ROIC and HgCdTe-based infrared detector technologies. The
20 current invention also eliminates the low yield indium bump and hybridization processes, thus significantly reducing the cost of the currently available infrared systems. A key advance in the modern solid-state technology is clean processing in order to prevent the contamination of sensitive surfaces so that the stability and reproducibility of device characteristics are improved.

Traditionally, the Si wafers were cleaned using wet chemical etching processes, such as the RCA process¹ (W. Kern and D.A. Puotinen, Cleaning solution based on hydrogen peroxide for use in silicon semiconductor technology, RCA Rev. 31, 187 (1970)) and the Shiraki processes² (Japanese Patent Application No. Sho. 63-46765) and a thermal cleaning in vacuum.

- 5 For the Si wafers to be ready for epitaxial growth they have to undergo a contaminant removal step as well as a surface passivation step. The contaminant removal step assures that the Si surface is clean and free of foreign elements (contaminants).

Surface contaminants can be classified as molecular, ionic and atomic. Molecular contaminants are typically carbo-hydroxides and carbo-hydrides originating in the mechanical
10 operations performed during the fabrication and handling of wafers. Organic solvent residues, grease or greasy films from containers are such molecular impurities held usually by weak electrostatic forces. Ionic contaminants are typically present after chemical etching, and can be physisorbed or chemisorbed onto the surface. Alkali ions are particularly harmful for epitaxial growth since they are known to give rise to different crystal defects. Atomic contaminants
15 include metals such as gold, silver and copper. Atomic impurities, especially the heavy ions, have a detrimental effect on the overall performance of the devices.

Once the contaminants are removed from the wafers, the bare Si atoms of the surface are highly reactive. Atoms lying on the surface have electrons that do not participate in the bonding with the bulk atoms, creating so-called dangling bonds. These dangling bonds represent
20 unsaturated conditions with a high potential energy. They tend to grab and form bonds with any available atoms and therefore re-contaminate the surface.

¹ (W. Kern and D.A. Puotinen, Cleaning solution based on hydrogen peroxide for use in silicon semiconductor technology, RCA Rev. 31, 187 (1970))

² (Japanese Patent Application No. Sho. 63-46765)

In order to prevent the contamination of these surfaces during further processing and/or handling (like the loading into the MBE chamber) a passivation step is necessary. This step is to passivate the ROIC surface on which the II-VI materials are to be grown subsequently and needs to be distinguished from the passivation of infrared devices fabricated on the II-VI layers by CdTe discussed later in this invention. This particular passivation step consists of a controlled deposition of a thin layer of oxide that can be removed by thermal heating to re-reveal the dangling bonds of the surface Si atoms. More particularly, the oxide layer is thermally desorbed at temperatures above 850°C in MBE growth chamber, thereby exposing a clean Si surface suitable for epitaxial growth. Importantly, the conventional approach requires thermal treatment of the Si wafer at a temperature above 850°C to remove the passivation layer. The performance of the ROIC will severely degrade if this high temperature cleaning process is adopted for the current invention of monolithic infrared detectors. One of the key aspects of the current invention is to prepare the ROIC surface at temperatures not exceeding 500°C, discussed as follows.

Moreover, the crystal quality of HgCdTe grown on conventional CdZnTe bulk substrates or CdTe thin films is detrimentally impacted by the substrate's surface quality. More particularly, the cleaning process results in an uneven surface due to the different etching (reaction) times of the various constituents (such as Cd vs. Te, or Cd vs. Zn). The HgCdTe crystal quality is affected by the defects that are formed at the interface during the nucleation. Moreover the contamination that is created by exposing the substrates to the environment is not entirely removed by the cleaning process. The presence of foreign atoms on the substrate creates nucleation centers for defects within the HgCdTe layers.

Read-Out Integrated Circuits (ROICs) are prone to failure at high temperatures. Consequently, applications requiring an opto-electronic device structure to be grown on an ROIC require that the entire process be carried out at temperatures below the maximum sustainable temperature of the ROIC, which is about 500°C. Conventional methods for preparing Si wafers
5 are not acceptable because they require a thermal treatment at or above 850°C.

Accordingly, a first object of the present invention is to provide a new two-step process for cleaning a silicon wafer.

Another aspect of the invention relates to an improved method for removing the oxide passivation layer created on the ROIC surface before the growth of II-VI layers commences.
10 More particularly, an object of the present invention is to provide a method for removing a passivation layer at a temperature below the maximum sustainable temperature of read out integrated circuits (500°C).

Yet another object of the present invention is to provide a high sensitivity monolithic infrared photon detector including a read-out integrated circuit fabricated on silicon and high
15 quality multi-layer HgCdTe ~~layers~~structures grown directly on the silicon/silicon-ROIC.

Another object of the present invention is to provide a monolithic interconnect between the detector contacts and the ROIC input gates involving a height difference of over 15 microns.

SUMMARY OF THE PRESENT INVENTION

An infrared sensing device is provided which includes at least one infrared detector containing at least one planar photovoltaic diode fabricated on a mesa-shaped II-VI semiconductor multi-layer structure produced by molecular beam epitaxy technique on a readout
5 integrated circuit, which is pre-fabricated on a special silicon substrate. At least one infrared detecting cell is formed in the mesa, with a conductive interconnect layer connecting the detection cell to the readout integrated circuit.

According to one aspect of the invention, the readout circuit (ROIC) that is needed for processing the signal generated by an infrared device is custom designed and fabricated in a
10 standard semiconductor foundry. In the prior art such ROICs are fabricated on (100) oriented silicon wafer in such a way that the ROIC could be joined to the infrared device containing plurality of detectors by indium columns formed on each detector. This process of joining the infrared device and ROIC device is called hybridization. The yield in these devices is poor due to the difference in the thermal expansion coefficients of the ROIC and infrared device at the
15 operating temperature of 77K and high-risk hybridization process. In this aspect of the invention, to enable defect-free II-VI semiconductors on silicon, the authors found that the ROIC needs to be fabricated on silicon substrates with one degree or the like tilted from the (100) crystal direction. This ensures twin-free growth of II-VI HgCdTe layers. Secondly, to preserve the circuits in the ROIC, a window free of any underlying circuits is provided for the subsequent
20 growth of II-VI layers. To fabricate a plurality of infrared detectors connected to the ROIC, the signal input gates covered with aluminum metal are provided in at least one row adjacent to the growth window. A second design to incorporate two rows of infrared detectors, the ROIC input gates are arranged in two rows on either side of the growth window.

According to another aspect of the invention, a procedure to prepare the ROIC surface at or below 500°C is provided. The authors have found that this is the maximum temperature to which the ROIC could be subjected during the II-VI material growth. In the prior art, to grow II-VI material by MBE, the substrates need to be cleaned at or above 850°C.

5 According to another aspect of this invention, the authors present the procedure to grow a multi-layer HgCdTe structure on the ROIC prepared according to the previous aspect of the invention. Due to the 19.3 % lattice mismatch between the silicon and II-VI materials, it was previously thought that II-VI layers ~~cannot be~~ could not grown on silicon. By employing the surface preparation outlined above and growing a CdTe buffer layer, the authors have achieved
10 single crystalline growth (the crystallinity is confirmed by the streaky RHEED (reflection high energy electron diffraction) pattern observed during the MBE growth) of at least one HgCdTe layer on the ROIC pre-fabricated on one-degree tilted (100) silicon substrates.

 According to another aspect of the invention, the authors fabricate a plurality of mesa structures containing at least one photovoltaic infrared detector that includes at least two layers
15 of Group II - VI semiconductor material having different band gaps. Each infrared detecting cell is electronically connected to the corresponding signal input cell in the ROIC. The wider band gap layer significantly reduces the surface passivation-related leakage currents in the infrared detector.

 According to yet another aspect of the invention, the signal output from each detector is
20 conductively connected to a ~~the~~ signal input cell of the ROIC. Since the detector output and the ROIC input cells are located in two different planes with at least 15 microns height difference, the authors fabricate a mesa structure at the edges of the growth window. Note that the photovoltaic junctions are planar junctions located on the top surface of one long mesa (of nearly

the dimensions of the growth window). The mesa structure at the edges of the growth window is constructed by a special etching in bromine-methanol solution. Each detector output cell is then connected to the plurality of ROIC signal input gates by individual metal electrodes running down the low angle slope of the mesa despite the large height difference between these two planes. The mesa has at least one sloped side on which a conductive trace connecting the detector output and the input of the readout integrated circuit is formed. Also, the detector common cell is connected to the ROIC common cell in a similar way.

BRIEF DESCRIPTION OF THE DRAWINGS

FIG. 1 shows ~~a the~~ unit cell for a cubic lattice and several crystal directions;

FIG. 2 is a schematic diagram of a silicon (211) surface;

FIG. 3 is a schematic diagram of a silicon (001) surface;

FIG. 4 shows a tilted (001) silicon surface;

FIG. 5aA is a physical diagram and 5bB is the energy band diagram of a p-n junction;

FIG. 6 ~~is the~~ shows a silicon (001) surface passivated with Hydrogen atoms;

FIG. 7 shows the silicon (001) surface of FIG. 6 after heating under ultra high vacuum (UHV); passivation is removed, and the dangling bonds are exposed;

FIG. 8 shows an over-etched (001) surface and the effect of over-etching the (111) facets;

FIG. 9 describes the prior art process for growth of MCT (FIGs. 9aA and 9bB) versus the newly proposed process (FIG. 9cC);

FIG. 10A shows the temperature profile for growth of MCT when using a single chamber versus (FIG. 10B) using a plurality of MBE systems;

FIG. 11 is a top view showing ~~the~~ infrared devices monolithically connected to the input gates of a readout circuit, according to one of the two design formats of the current invention;

FIG. 12 is a cross-sectional view of a monolithic infrared device shown in FIG. 11;

FIG. 13 is a top view showing two linear arrays of infrared devices monolithically
5 connected to the input gates of the custom designed readout circuit in accordance with ~~the~~
another embodiment of the present invention;

FIG. 14 is a cross-sectional view ~~taken substantially along lines 110-110~~ of the
monolithic infrared device shown in FIG. 13;

FIGs. 15(A) to 15(L) are cross sectional views corresponding to FIG. 14 showing
10 respective steps in the process for producing the prior art infrared imaging device;

FIG. 16 is a cross-sectional view showing a second prior art infrared imaging device
(Method-A);

FIG. 17 is a cross-sectional view showing a second prior art infrared imaging device
(Method-B); and

15 FIG. 18 is a cross-sectional view showing a third prior art infrared imaging device
(Method-C).

DETAILED DESCRIPTION OF THE INVENTION

A technology for producing a plurality of infrared sensing elements in a monolithic array
format is provided. Each element has a multi-layer structure of mercury cadmium telluride
20 (HgCdTe), a group II-VI semiconductor grown by MBE on a pre-fabricated silicon-ROIC. The
infrared sensing devices of the present invention are individually and monolithically connected
to the signal input cells of a readout electronic circuit (ROIC). In other words, both the infrared

sensing elements and the read-out electronics are fabricated on a common silicon substrate. The monolithic connection of the present invention eliminates the need for conventional columnar indium metal electrodes and the low-yield hybridization process (needed to interconnect the detector chip and the ROIC chip) by the direct growth of the complex HgCdTe structure on pre-fabricated read-out electronics on a common silicon substrate by Molecular Beam Epitaxy (MBE).

The present inventors have discovered that Silicon (Si) covered by a thin buffer layer film of, for example, CdTe (cadmium telluride) is a viable alternative substrate to bulk CdZnTe. Specifically, they have discovered ~~invented~~ that a readout circuit (ROIC) pre-fabricated on silicon can be used as substrate for CdTe buffer and subsequently HgCdTe detector layers growth by MBE resulting in "monolithic infrared detectors". The authors have found that the maximum sustainable temperature of the ROIC during cleaning and the growth is 500°C. Consequently, they have developed a process ~~cycles to~~ having the steps of: "pre-growth cleaning of the ROIC, passivateing with Hydrogen, remove passivation under safe conditions, growing a CdTe buffer ~~growth~~ and growing at least one HgCdTe layer".

Current growth techniques of HgCdTe on Si (~~FIG. 9a-2~~) (layer 2 in FIG. 9A) use two separate MBE systems, one that will allow the growth of CdTe thin films 1 on silicon (FIG. 9a-~~4~~) that will become a substrate 3 for growth in the second chamber (FIG. 9Bb-~~3~~). The newly formed substrate 3 is suited for growth after undergoing a typical substrate cleaning procedure. HgCdTe (~~FIG. 9b-4~~) layer 4, FIG. 9B) is then grown in the second system.

One aspect of our invention offers the alternative to use one chamber only, capable of carrying the necessary charge sources. The growth will then be involving a buffer layer 6 (FIG. 9C-~~6~~) grown on Si layer 5 (~~FIG. 9c-5~~), followed by the growth of HgCdTe layer 7 (~~FIG. 9c~~

7). The growth schematics for the two processes are shown in FIGs. 10Aa and 10Bb. FIG. 10Aa shows the substrate temperature profile for the growth using one MBE system versus (FIG. 10Bb) using two separate systems.

After the aforementioned clean-growth processes, the authors developed infrared devices monolithically connected to the underlying ROIC. The current invention couples the high performance of silicon signal processing readout circuits (Si-ROIC) with HgCdTe-based infrared devices.

Two different designs for the monolithic infrared detector arrays are illustrated here. In the first design format (FIGs. 11 and 12), a linear array of infrared detectors containing planar photovoltaic junctions are fabricated on a mesa formed in the II-VI material that ~~grows~~ is grown between the detector output cells and the ROIC input cells. Each detector output is then monolithically connected to the ROIC input cells by conducting lines flowing down the mesa slope.

The output of each detector (14 in FIG. 11) is monolithically interconnected to a corresponding signal input gate defined by the row of metal pads 1122 (FIG. 11) and the detector common 23 is fabricated as a long strip along the length of the ROIC 1111 and is monolithically interconnected by interconnect 28 to the ROIC common contact pad 1115. In the second design format (FIGs. 13 to 15) a mirror image of the previous design is added to the circuit in the y-direction (vertical in the page) giving rise to simultaneously producing two similar linear arrays, which if needed could be separated by cutting along the center line 110-110 (FIG. 13). The entire process of fabrication of devices in these two formats is essentially the same and is illustrated in FIGs. 15A-15L, for the second design format device.

The enormous lattice mismatch between the silicon (the substrate for the ROIC) and HgCdTe layers (for infrared detection) is overcome by the growth of a CdTe buffer layer. The growth of CdTe(111)B (where B represents the polarity of the molecular arrangement, i.e., Te terminated surfaces) can be performed successfully on Si(001) tilted around 1° off axis. The tilt
5 of the surface orientation enhances the correlation between seeds and suppresses twin crystal formation, leading to a single crystal film. A schematic diagram of such a surface is shown in FIG. 4.

For a tilted (001) surface the morphology shows terraces and additional steps spaced out to accommodate the surface tilt. The tilted surface induces a larger number of steps on the
10 surface, and these steps are beneficial for the growth of twin-free single crystal material.

The silicon (Si) substrate, which is rather inexpensive, offers a rugged, stable mechanical support for the entire structure. Moreover, the Si substrate can carry an additional microelectronic device enabling further integration with the devices to be fabricated onto MCT. More particularly, according to the present invention MCT detectors are monolithically
15 integrated with Si Read-Out Integrated Circuits (ROICs), providing substantial benefits over conventional techniques in which ROICs are hybridized onto MCT detectors using Indium bumps.

Similar results may also be achieved by combinations of buffer layers other than CdZnTe and other II-VI semiconductor layers for infrared absorption. The p-n junctions in a device
20 formed according to the present invention are planar and are totally buried under a wide band gap HgCdTe layer achieving very high dynamic impedance and sensitivity.

An aspect of the present invention relates to a procedure to clean ROIC-Si(001) in preparation for epitaxial growth of semiconductor films by MBE. The semiconductor films are

grown on a vicinal or off-angle silicon wafer, at a temperature below the maximum sustainable ROIC temperature of 500°C.

Si-ROICs are commercially suitable for hybridization. A modified ROIC according to the present invention includes a circuit fabricated on a silicon wafer having a tilted orientation and having a window uncovered by previously fabricated circuits, that will be used for growth of detector material is described herein. Growth of II-VI semiconductor material on Silicon wafers with built-in ROICs can be performed on various Si orientations, like (211), (111), nominal surfaces or off-axis.

Si(001) wafers have been considered the most widely used semiconductor material for fabrication of various advanced electronic devices and as substrates for the growth of many homoepitaxial or heteroepitaxial layers, such as Si/Si, SiGe/Si, GaAs/Si, ZnSe/Si and CdTe/Si. For all these epitaxial structures, a clean Si substrate has to be prepared prior to the onset of the epitaxial growth. A large number of contaminants present on the Si surface can prevent the growth of single crystalline material, while a reduced number of contaminants results in the growth of an epilayer with a commensurate level of defects. Ideally, all contaminants are removed in order to obtain reliable and reproducible results.

Prior to applying the methods described in the current innovation, the surface of the Si(001) wafer must be cleaned and passivated. More particularly, the wafer may be cleaned using a conventional wet chemical method or the like in order to obtain an atomically clean surface.

Alternatively, the wafer may be cleaned using an oven containing a source of ozone, such as a Mercury lamp. The ozone generated in the oven will react with the wafer contaminants and reaction products will be removed. However, the use of low temperature cleaning process is preferred, because the components in the ROIC degrade if subjected to temperatures >500°C.

To prevent recontamination, it is necessary to cover the freshly cleaned surface with a thin oxide to passivate any dangling bonds on the cleaned surface. Moreover, this oxide layer needs to be removed in-situ in the MBE chamber before the CdTe buffer layer growth starts.

5 A first aspect of the present invention relates to a two-step etching process for removing the oxide layer selectively from the growth window 6 shown in FIGs.11, 13 and FIG.15a. First, the wafer is wet etched in a diluted solution of HF:H₂O (2-10%) for 50 to 80 seconds. The water used in the wet etch solution should be deionized water with above 18 megaohms resistivity. The first etching step must be sufficient to effectively remove the oxide layer previously formed.

10 After the first etching in HF solution, the wafer is slowly pulled out of the solution and immediately submerged into concentrated NH₄F (20%-40%). The period of time during which the ammonium fluoride etch is performed is critical. A short exposure leaves an uncovered silicon surface, sensitive to future contamination, and most of the hydrogen passivation/termination is in the form of mono- and trihydrides. A long etching time in NH₄F produces rough surfaces with (111) facets covered by monohydrides. This second wet etch will
15 yield a dyhdride terminated, smooth Si(001) surface for etching periods of 30 +/- 10 seconds. The dyhdride terminations provide a passivation layer. (FIG. 6)

Etching of the ROIC 4111 with open windows 6116 that expose the silicon can be performed either by dipping the entire wafer into chemicals or by dispensing onto the wafer certain amounts of chemicals while it is spinning. The growth window is rectangularly 112
20 defined along the length of the ROIC 111 and covers the area between the two rows of ROIC pads 2,3112,133 as shown in FIGs. 413 to 15A. This window consists of a clean silicon surface after the procedure described above is performed.

To produce the monolithic infrared device, two embodiments consisting of two different design formats are presented in this invention. The first design shown in FIGs.11 and 12 consists of a linear array of planar photovoltaic infrared detectors fabricated on a mesa formed in the II-VI material structure in window 6116. The detector outputs 26126 and the detector common 23 are monolithically connected (~~29 and 28~~respectively by interconnects 29 and 28) to the corresponding input gates of the ROIC (FIG.11). The signal input gates 2112 of the ROIC are arranged in a row on the topside of the growth window as illustrated in FIG.11. The detector common ~~contact~~region 23 is defined as a long strip parallel to the row of detectors ~~(14 in~~ (FIG.11) on the mesa and later conductively connected by interconnect 28 to the ROIC common pad 115.

The second design format consists of two rows of ROIC signal input gates arranged on either side (top and bottom) of the growth window as illustrated in FIG.13. In this format, the plurality of detectors is fabricated in two adjacent rows (with the detector common running at the center between the two rows of detectors FIG.13). The output 126 of one row of detectors ~~26-14~~ are connected to the top row of signal input gates 2112 of the ROIC ~~+111~~, while the output 27 ~~that of the second row of detectors~~ 27 15 are connected to the corresponding input gates 133 in the bottom row ~~3-(as~~ as illustrated in FIG.13). As before, the detector common 23 is conductively connected by interconnect 28 to the ROIC common pads 5115, 24. The rest of the details and procedure for the growth of infrared detecting layers and fabrication of detectors are same in both embodiments.

The step-by-step procedures common to both design formats for the growth and device fabrication is illustrated in FIGs.15A-L as an example, for the second design format. The FIGs.11 and 13 show a part of the custom designed ROIC in the two formats. On the top and

bottom side of these figures, the rest of the signal processing electronics are arranged (not shown since they do not concern the current invention). Also these figures show only a few of the detectors of the total 256 detectors in one row (the first design, FIG.11) or 512 detectors in two rows (256 in each row, the second design FIG.13) connected to the ROIC. The corresponding cross sectional views of one of the detector element are shown in FIGs. 12 and 14 respectively for the two design formats, respectively.

The entire process of monolithic infrared detector array fabrication involves three major steps:

1. The design and the subsequent fabrication of the ROIC in a foundry. Usually, the custom-designed ROIC is encapsulated with a protective silicon nitride or silicon dioxide layer at the end of the ROIC fabrication.
2. The growth of multi-layer CdTe/HgCdTe structure selectively in a window 6116 on the ROIC 4111. A window 6116 where the encapsulant layer is removed and the silicon surface free of underlying circuits is prepared before the growth of CdTe/HgCdTe structure. Though the CdTe/HgCdTe structure grows on the entire ROIC, only that portion that lies within this window is single crystalline material suitable for the subsequent detector fabrication.
3. The fabrication of plurality of infrared detectors conductively connecting each detector signal output to the corresponding input gates in the ROIC. The detector common 23 is connected to the ROIC common contacts 115, 24 5—in a similar way, thus completing the monolithic infrared detector array. Also, this invention describes two design formats for the monolithic infrared detector array as discussed earlier and describes a method to achieve monolithic interconnects despite the large height

difference between the two planes consisting of the detector outputs and the ROIC inputs.

Turning to the growth of infrared material on ROIC and detector fabrication, the first step is to open a window free of the encapsulant layer discussed earlier in the ROIC 4111. As shown in FIGs. 15(a)A-B, before the HgCdTe is grown on the Si-ROIC 4111, a buffer layer 1577 of single crystalline CdTe is formed within a window 6116 in the encapsulant layer 4154 on the ROIC 4111. Specifically, the ROIC 4111 is loaded into an ultra high vacuum system chamber, and the growth window 6116 is stripped of the passivation layer to expose the clean silicon surface and a buffer layer 7-157 is grown across the ROIC substrate 4111 according to the Si crystalline orientation. The buffer layer can be any II-VI compound or materials of similar structure (Arsenic, Phosphorous, Germanium, Antimony) or compounds selected from the group (CdTe, ZnTe, HgTe, HgCdTe, ZnSe, ZnSSe, and CdZnTe).

Once, the substrate is thermally cleaned inside the chamber and a proper elemental Si surface (in the growth window 6116) is observed by reflection high-energy electron diffraction (RHEED), the CdTe growth is initiated.

More particularly, after the removal of the passivation 4layer 154 (FIG.15a) from the growth window 6116, the substrate is cooled under Arsenic flux from 500°C to 400°C, followed by a cooling under CdTe flux from 400°C to 350°C. Next, the substrate is cooled down to 210°C and CdTe is deposited at this temperature for about 2 minutes. The substrate is then heated to about 310°C under Te flux and from 320°C to 350°C under Te and CdTe fluxes. The substrate is kept at 350°C for 10 minutes under CdTe and Te fluxes. Next, the substrate is cooled to about 310°C under Te flux. At this temperature additional 4-8 microns of CdTe are grown with CdTe flux that assures a growth rate of about 2Å/second.

After this process, the sample is cooled to the HgCdTe nucleation temperature of about 180°C and allowed to stabilize for about an hour under no material flux. The HgCdTe growth process is then initiated. First the grown CdTe surface is exposed to the Hg flux. The flux is adjusted such that the chamber pressure is around 2.0×10^{-5} Torr. Next, a Te flux is provide for about 10 seconds followed by a subsequent exposure to CdTe. The Te and CdTe fluxes are adjusted so that their ratio provides the growth of HgCdTe with desired composition. During the growth the surface is always exposed to Hg, Te and CdTe fluxes. The substrate temperature is ramped down during the growth of HgCdTe to compensate for the heat absorption into HgCdTe layer, as it grows. The HgCdTe growth process takes approximately 4 hours, and the entire growth time, from loading to unloading, takes about 20 hours. The result is shown in FIG. 15**B**.

In FIG. 15**B**, once the buffer layer 7157 grown, the growth of HgCdTe commences. It should be noted that, depending on the buffer material used, a waiting period may be necessary prior to MCT growth. The waiting period being defined by the difference between the growth temperature of the buffer and the growth temperature of the HgCdTe layer, and by the system ability to adjust to the new temperature setting.

During the waiting period the buffer layer may be exposed to specific fluxes (like Tellurium, Mercury, others) in order to prevent any material or specific atomic species from desorbing.

The details of the device and the fabrication process are described as follows. FIG. 11 is a top view of a monolithic ROIC/HgCdTe detector cell array according to the first of the two designs presented in this invention. Si-ROICs are commercially suitable for hybridization. A modified ROIC according to the present invention includes a circuit fabricated on a silicon wafer having a tilted orientation and having a window 6116 uncovered previously to the II-VI material

growth on the ROIC 4111. Growth of II-VI semiconductor material on Silicon wafers with built-in ROICs can be performed on various Si orientations, like (211), (111), nominal surfaces or off-axis. At the end of the manufacturing process of the ROIC, the entire ROIC 1 is covered with silicon nitride or silicon dioxide encapsulant (4154 in FIG. 15a, shown partially after selectively etching it from the growth window). A window 6116 is etched in the custom designed ROIC 1 in a region that is free of any underlying circuits (see FIGs. 11 to 15). A part of the ROIC relevant for the growth of HgCdTe material and subsequent device fabrication is shown here. On either end (top and bottom), the rest of the readout circuits including the shift registers for the signal processing ~~is~~are distributed (not shown here).

FIG. 12 is a cross-sectional view of FIG. 11 ~~taken substantially along line 110-110 of FIG. 13.~~

In the first design, the ROIC 4111 is provided with a plurality of signal input gates in a row 2112, each covered with aluminum metal. The size of the alternate plurality of pads 2112 is relatively large, 75x100 microns, to facilitate bonding to a test board (not illustrated) and statistical testing of the infrared detectors. Referring to FIG. 15(a)A, a window 6116, clear of any underlying ~~circuit~~ circuitry, is provided for the subsequent growth of infrared sensitive material. A protective layer of silicon nitride (not shown) covers the entire ~~ROIC surface of ROIC 1114~~ except the bonding pads 112, 133 ~~2,3~~ (FIGs. 11, 13 corresponding to the two designs) as discussed earlier. Prior to the HgCdTe growth, the protective layer is selectively removed in the growth window 6-116 by performing the standard photolithography technique. The wafer is then loaded into an ultrahigh vacuum MBE chamber. The surface preparation and growth of CdTe buffer 7157, HgCdTe layers 8,9 and ~~the a~~ CdTe cap layer 10 structure are carried out in accordance with the previously described procedure.

A first buffer layer ~~7~~157 approximately 5 to 8 microns thick of CdTe is disposed on the ROIC ~~4~~111 by MBE to reduce the lattice mismatch between silicon and the subsequent layers of HgCdTe.

5 A first layer 8 of HgCdTe, about 10 microns thick, with narrow band gap, is deposited by MBE on the buffer layer ~~7~~157. The band gap of the HgCdTe 8 is selected in accordance with the desired cutoff wavelength of the detector.

A second HgCdTe layer 9 with wider band gap (compared to the previous HgCdTe layer 8) and about 1 micron thick is then deposited, followed by the deposition of a thin CdTe layer 10 for protection of the entire structure.

10 Both the HgCdTe layers 8 and 9 are doped with indium during the growth to make the electron as the dominant current carrier (n-type). The entire sample is then coated with a 5 micron thick photoresist layer 11 (FIG. 15C). A plurality of windows 12 and 13 (FIG.15c) (in the case of the first design format only the windows 12 are present, ~~ref=~~refer to FIG.11) are then selectively opened in this photoresist 11 by photolithography, a common technique known to
15 everyone familiar with this art.

The plurality of p-n junctions(14 in FIG.11 for the first design and 14,15 in FIG.13 for the second design) is then fabricated by implementing arsenic atoms through these windows 12 (and 13 in the case of second design) selectively by an ion implantation technique. Ion implantation is one of the standard techniques to change the polarity of the electrical conduction
20 in selected regions in a semiconductor. After opening windows in the 5 micron thick photoresist 11, arsenic ions are implanted with 350 keV energy and a dose of $1 \times 10^{14} \text{ cm}^{-2}$.

Due to the high initial energy (350 keV), arsenic travels through the entire thickness of HgCdTe layer 9 through the windows 12 (and 13) and forms a p-n junction in the n-type

HgCdTe layer 8 once the arsenic atoms (a p-type dopant in HgCdTe) are electrically activated as described below. Outside of window 12 (and 13) the photoresist 11 prevents the implanted arsenic entering in to the HgCdTe layers thus achieving selectivity. The implanted arsenic atoms by themselves are not electrically active.

5 A post-implant annealing is performed to activate these arsenic atoms to change the conductivity in regions 14,15 to p-type. The layered, selectively implanted ROIC 4111 is then annealed in an ampoule containing mercury overpressure to activate the arsenic. The ampoule contains two compartments with a constriction in between. The sample is placed in the top compartment while a tiny droplet of mercury is placed in the bottom. Due to the high vapor
10 pressure of mercury, the top compartment is under mercury over pressure. A tiny droplet of mercury provides enough overpressure to avoid any outdiffusion of mercury from the sample surface.

 The mercury over pressure is necessary to avoid the creation of vacancies in the multi-layer HgCdTe structure by outdiffusion of mercury atoms. The annealing is done in three steps:
15 425⁰C, 10 minutes; 300⁰C, 12 hours; 235⁰C, 12 hours. This annealing gives rise to about 10¹⁷/cm⁻³ hole carriers in the arsenic doped regions 14,15 and about 10¹⁵/cm⁻³ electrons in the indium doped n-type HgCdTe layers 8 and 9. The plurality of junctions 14,15 is now capable of collecting the electron hole pairs (signal) generated by the incident infrared radiation by the built-in potential difference at the junction due to opposite conducting polarity on either side of
20 the junction.

 After the annealing, the masking photoresist layer 11 is removed in acetone and the sample is thoroughly cleaned in methanol, followed by DI water. In the next step, the grown infrared material structure in the window 16 (FIG.15dD) is selectively protected by 5 micron

thick photoresist 151 while the material from rest of the areas on ROIC 111 is removed. After protecting the wanted areas 16, the removal of the material from other areas could be accomplished using standard dry etching techniques or by chemical etching in 2% bromine in hydrobromic acid in about 3 to 5 minutes. This leaves the infrared sensitive HgCdTe material structure in the original growth window 116 but removes the material from unwanted areas and exposes the ROIC contact pads 123 as shown in FIG. 15dD.

In the next step, the material on windows 17 that ~~is~~ are dimensionally within the windows 16 is protected as before, leaving the rest of the areas 122 open. Then the entire sample is dipped in 4% bromine in hydrobromic acid solution for a few seconds. This produces a mesa structure (FIG. 15eE) with a 40 to 50 degree angle 19 between slope 18 (mesa side walls) and the surface of ROIC 111 (horizontal plane).

The formation of the slope in the mesa structure can be better visualized by comparing FIG. 15dD and 15eE. The reason for the formation of slope is as follows. Due to the residence time of the etching chemical and the high concentration, the top layers in the strip of material structure that lies between the windows 16 and 17 gets etched first. As the etching proceeds to remove the bottom layers, lateral etching occurs in the region where the top layer once was resulting in a sloped side 18 (FIG. 15eE).

The photoresist 151 is then washed off in acetone. The entire sample is then dipped in 0.05% bromine in methanol solution for about 20 seconds. This removes the CdTe cap layer from the top surface of the mesa. A thin CdTe layer 20 (1000 angstrom thickness) followed by 2000-angstrom thickness of ZnS 21 are then deposited on the surface of the sample for passivating and protecting it. The cross sectional view of the device at this stage is shown in FIG. 15fF.

One of ordinary skill in the art will appreciate that standard methods like thermal or electron beam evaporation may be used in place of MBE to deposit these CdTe 20 and ZnS 21 layers. Note that the layer 20 and 21 also covers the ROIC contact metal pads 2112 and 3133. In the next step the CdTe 20 and ZnS 21 are removed from the ROIC contact metal pads selectively
5 by protecting the entire mesa structures with photoresist by performing photolithography. The exposed CdTe 20 and ZnS 21 on the ROIC input metal pads are etched off typically in about 40 seconds by dipping successively in buffered hydrofluoric acid (20 sec) and buffered hydrochloric acid (20 sec) (FIG.15gG).

In the next step of photolithography, a window 22 is opened (FIG ~~43-h~~15H) in the
10 protective photoresist and the ZnS 21, and CdTe 20 layers are removed selectively in this window 22, to facilitate contact metal deposition for detector common contact with the HgCdTe layer 8. Another step of photolithography is done to deposit indium metal 23 of thickness about 1000 angstroms selectively in window 22 by a lift-off technique (FIG. ~~43-i~~15I). Then contact windows 24124, 25 for the p-regions 14 and 15 are selectively opened (FIG. ~~43-j~~15J) and 1000
15 angstrom thick gold metal ~~26126,27127~~ deposited in exactly the same way as the common contact was made in the previous step (FIG.15-kK).

The last step in the device processing is to connect the signal output gates ~~26126,27127~~ from each detector to the signal input gates 2112, 3133 of the ROIC and similarly the detector common 23 to ROIC common pad 1155. This is a very critical step because the ROIC metal
20 pads ~~2,3,5~~112,133,115 and the detector contact metal pads ~~26,27,126,127,23~~ are located in two different planes involving a height difference of about 15 microns or more. The interconnecting metal lines 28,29,30 (FIGs.11 to 14) will break due to the height difference if a slope to ensure good step coverage is not fabricated prior to the interconnecting metal deposition.

The invention is to fabricate the mesa structure with the side walls sloped by 40 to 50 degrees with respect to the ROIC surface plane, as described earlier in reference to FIGs. 15d and 15e. According to this aspect of the invention, a method is disclosed for overcoming this barrier problem associated with connecting the detector outputs 26126, 27127 to ROIC input metal pads 2, 3112, 133. The same applies to the conducting line 28 connecting the ROIC common contact 5115 and the detector common contact 23. The interconnecting lines are defined photolithographically and consists of 0.05 micron thick titanium followed by 0.1 micron thick gold. The present inventors have discovered a reliable, cost-effective method for connecting the detector output metal pad 26126 (and 27127) to ROIC input 2112, 3133 (and 3133) by fabricating a low angle 19 slope/ramp 18 in the HgCdTe material lying between the regions 16 and 17. The cross section of the final device (in the second design format) is shown in FIGs. 14 and 15L).

As described earlier, the multi-layer material 122 that grows between a detector cell area 17 and the ROIC area 16 (see FIG. 15(e)) is used to fabricate a low angle slope. Notably, selected portions 17 of the mesa 47 are protected with photoresist, and the unprotected regions are etched in a bromine-hydrobromic (HBr) acid solution or the like. Preferably, 4% bromine in HBr acid is used. The etching is done typically for a few seconds.

Due to the fast etching characteristics of this solution and its isotropic etching characteristics, considerable undercutting (due to lateral etching in the top layers while the etching proceeds vertically in the bottom layers) is achieved in the material 122, giving rise to a low angle slope as described earlier. The fast etching characteristics leads to considerable lateral etching in the top layers while the bottom layers in the material 122 are being etched in the

vertical direction leading to a sloped wall instead of a vertical wall (which will be the case if no lateral etching occurs in the top layers) in the mesa structure.

The interconnections 29,30 between the detector output gates ~~26,27~~126,127 and the corresponding ROIC input gates 2,3 are fabricated by depositing a titanium-gold bi-metal layer
5 by a conventional photolithographic lift-off technique. Similarly, the metal electrode 28 connects the detector common 23 and ROIC common ~~5~~115. First a titanium layer of about 400 to 500 angstrom is deposited followed by about 1000 angstrom of gold in the same evaporation run without breaking the vacuum. This low angle slope, which can be on the order of 40 to 50 degrees with respect to normal (perpendicular to the ROIC surface), is critical in ensuring proper
10 step coverage when metal is deposited between the detector output and the ROIC input. In the same fabrication step, a similar conductive, monolithic interconnect 28 between the detector common 23 and the ROIC common contact ~~5~~115 is also established (the cross sectional view is shown in FIG.15 ~~k~~K).

A method for simultaneously producing two linear arrays per die will be disclosed with
15 reference to FIGs. 13 and 15. The fabrication details described above are same in this design too and hence described briefly as follows.

FIGs. 13 and 14 show the top view and the cross-sectional view, respectively, of an array of devices in accordance with the second embodiment. The process sequence to produce this cell array is shown in FIGs. ~~15(a)A~~ to ~~15(k)K~~.

20 The protective layer ~~4~~154 of silicon nitride or silicon dioxide layer is selectively removed from the growth window ~~6~~116 by lithography as shown in FIG. ~~15(a)A~~. The ROIC wafer ~~4~~111 is then inserted into the high vacuum chamber of a MBE system and the surface prepared at or below the maximum sustainable temperature of ROIC 111 in the manner previously described.

The material structure involves a series of layers 7157, 8, 9 and 10 as before.

A plurality of p-regions is selectively implanted as shown in FIG. 15(e)C. The difference between this embodiment (FIG.13) of the invention and the previous one (FIG.11) is that the design and fabrication incorporates two similar linear arrays of detectors monolithically connected to two rows of ROIC inputs 2,3112,133 (FIG.13) instead of only one row of detectors and input gates in the ROIC (the mirror image plane between the two designs is shown along the line 110-110 in FIG.15kL. This leads to significant cost saving and technical advantage in imaging applications. Preferably, the p-regions are formed by implanting arsenic with a 1×10^{14} cm^{-3} dose at 350 keV energy, followed by thermal annealing under mercury overpressure at 425⁰C for 10 minutes, 300⁰C for 12 hours and 235⁰C for 12 hours, as described before with reference to the first design. However, other methods like in-situ doping, diffusion of dopants like arsenic, gold, etc. will also yield the same desired results. The thermal annealing electrically activates the impurity species. This procedure also enables the formation of the actual electrical junction in the HgCdTe layer 8 by the diffusion of arsenic atoms through the HgCdTe layer 9.

Next, the II-VI material lying on the ROIC contact pads 2,3112,133 is etched away as shown in FIG. 15(~~d~~)D.

The material 122, being the difference between the regions 16 and 17, is then chemically etched to form a slope as shown in FIG. 15(e)E. The fabrication procedure for this slope and the monolithic metal interconnects are the same as previously described for the arrays shown in FIG.11.

The thermal process used to activate the impurity species degrades the interface between the CdTe layer 10 and HgCdTe layer 9. Consequently, the previously grown CdTe cap layer 10

is removed by etching in 0.5% bromine in methanol for about 20 seconds and a fresh CdTe layer 20 and ZnS cap layer 21 are deposited (FIG. 15(f)).

In the next step of photolithography, the CdTe 20 and ZnS 21 from the ROIC contact pads ~~2,3~~112,133 are etched (FIG.15gG), exactly as described before. A detector common contact window 22 is then opened by photolithography (and the CdTe 20 and ZnS 21 are removed to enable contact to HgCdTe layer 9 [FIG. 15(h)H].

FIG. 15I(i) shows the device after the deposition of indium metal for the detector common contact defined by another photolithography step. Similarly contact windows 24,25 to the two rows of p-HgCdTe regions 14,15 are opened by performing another lithography step and gold metal ~~26,27~~126,127 of ~~thickness~~ 1000 angstrom thickness deposited as shown in FIGs. 15J(j) and 15K(k).

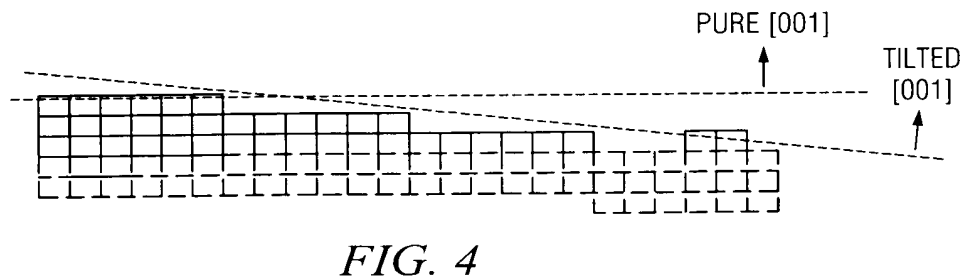
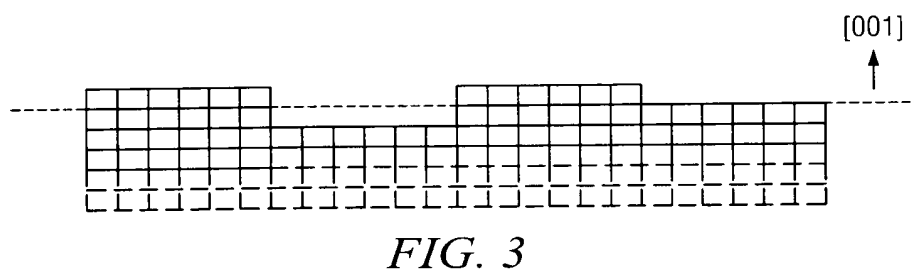
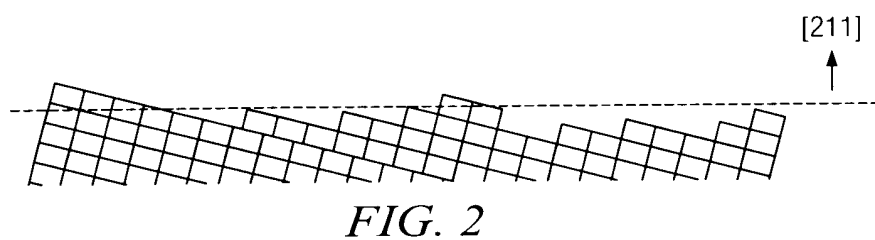
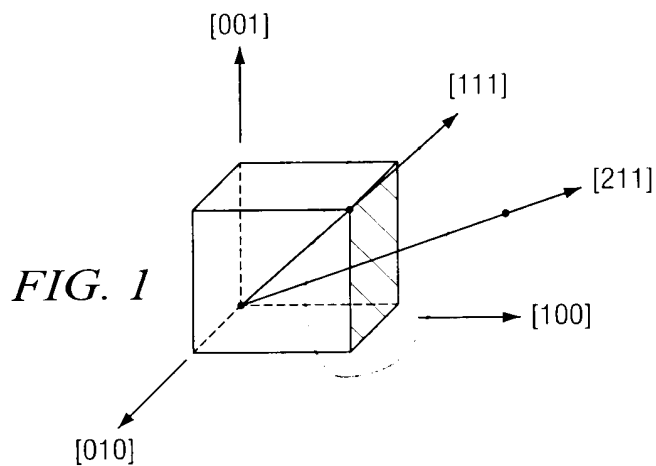
FIG. 15(L) shows the final step of fabricating a monolithic metal interconnect ~~15~~28, 29, 30 by depositing a titanium and gold bi-layer. Either lift-off or selective metal etching could be done to accomplish this step, although liftoff is the preferred mode for this step.

While various embodiments of the present invention have been shown and described, it should be understood that other modifications, substitutions and alternatives could be made without departing from the spirit and scope of the invention, which should be determined from the appended claims.



Attachment D
Marked-up Copy of Drawings

1/7



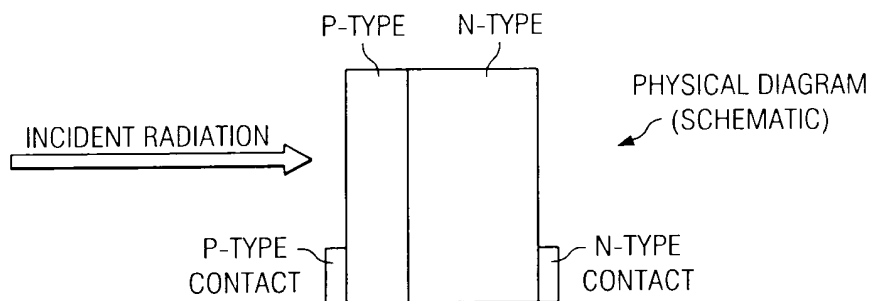


FIG. 5A

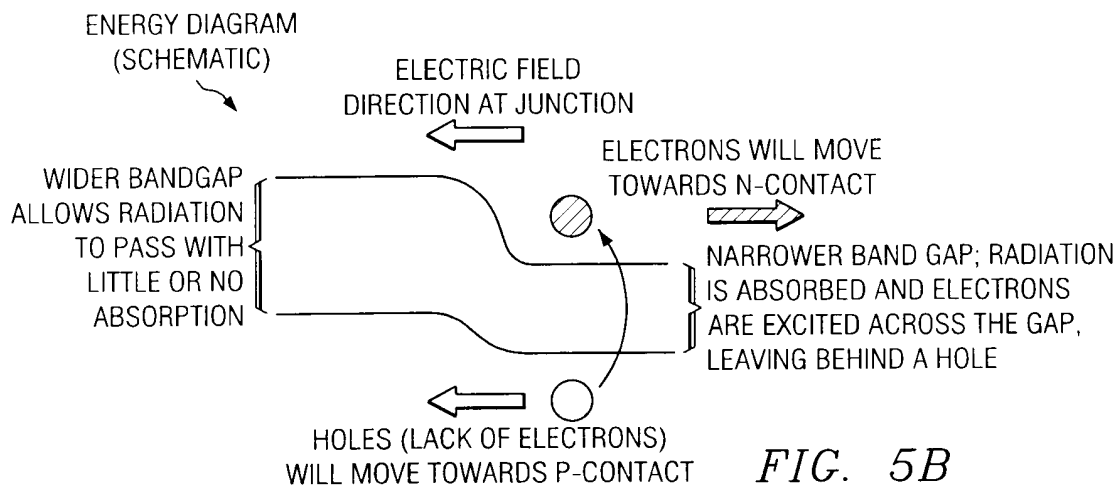
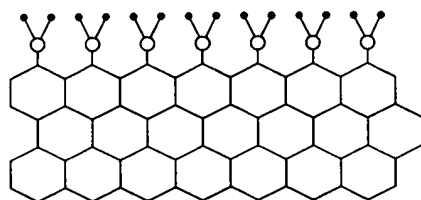


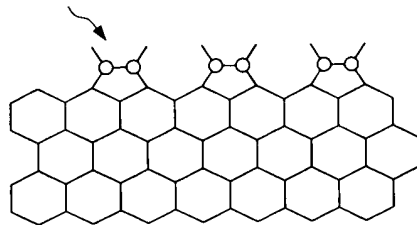
FIG. 5B



• HYDROGEN ATOM
○ Si SURFACE ATOM

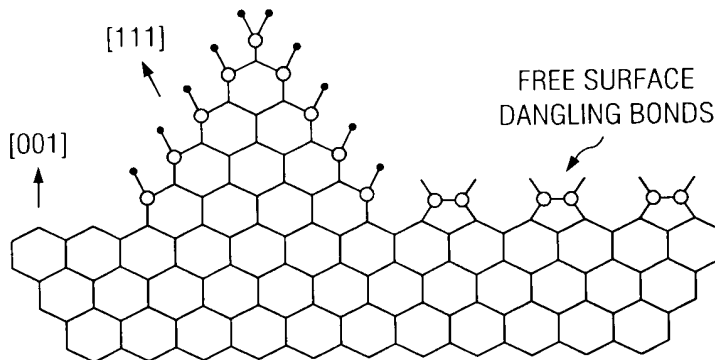
FIG. 6

FREE SURFACE
DANGLING BONDS



○ Si SURFACE ATOM

FIG. 7



• HYDROGEN ATOM
○ Si SURFACE ATOM

FIG. 8

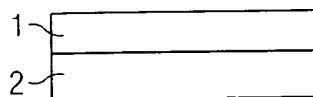


FIG. 9A
(PRIOR ART)

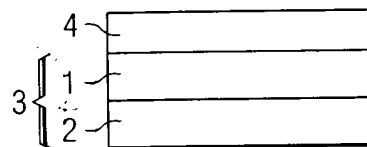


FIG. 9B
(PRIOR ART)

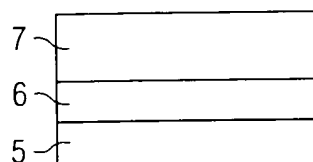
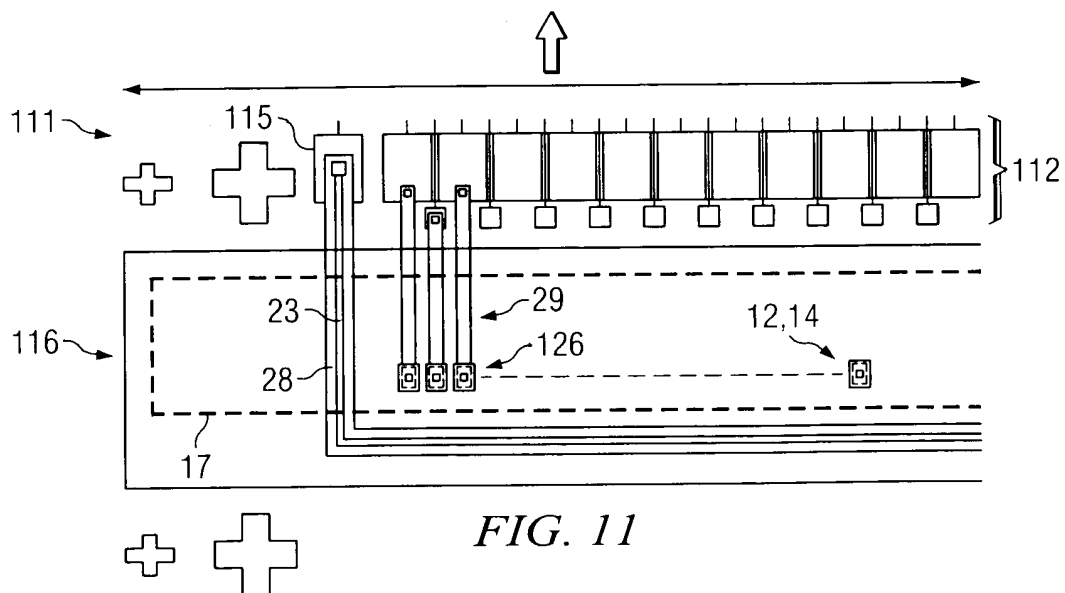
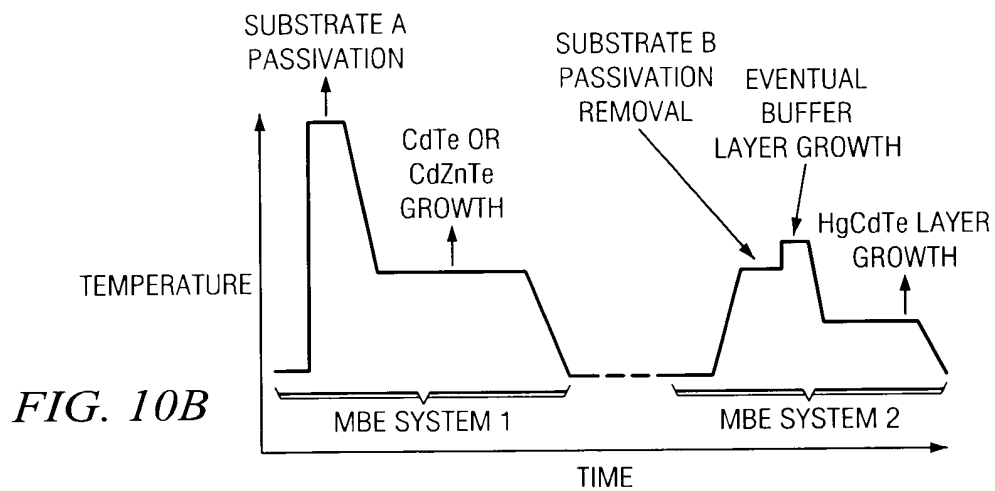
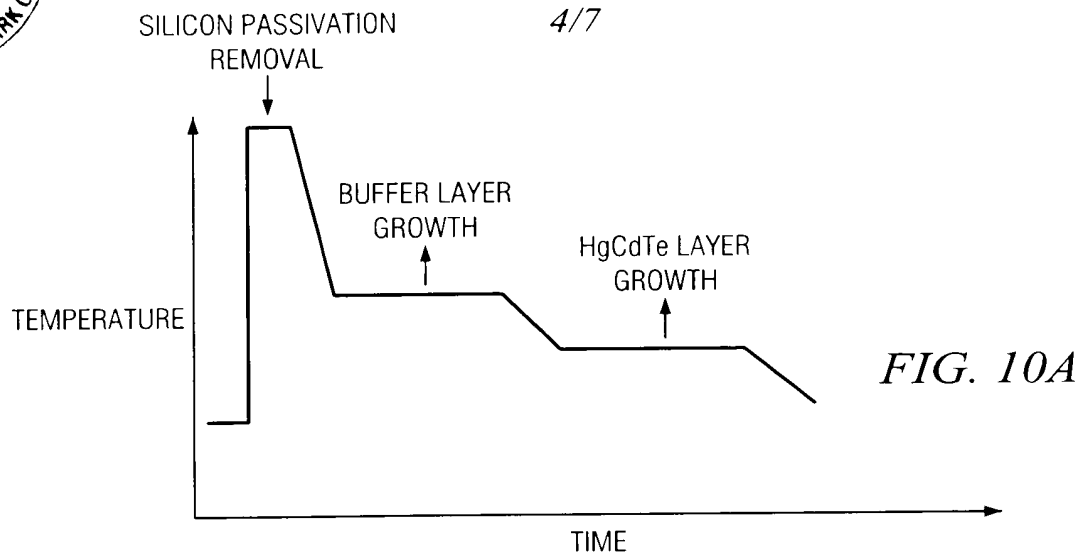
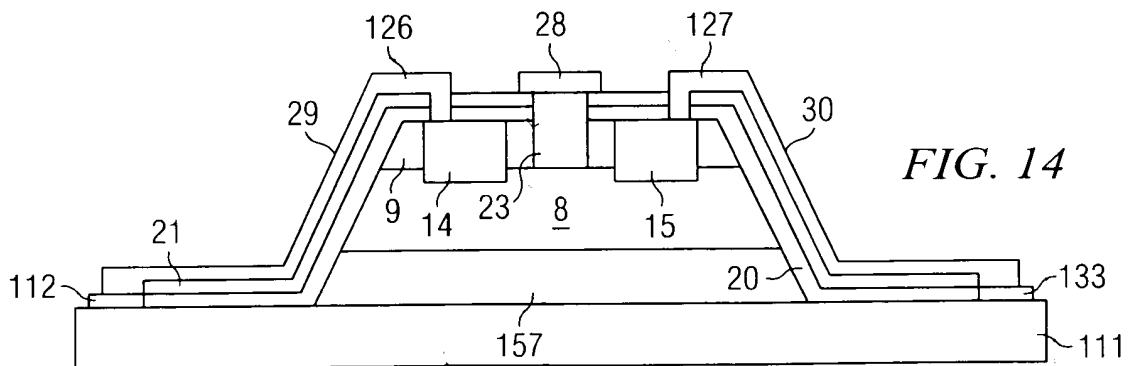
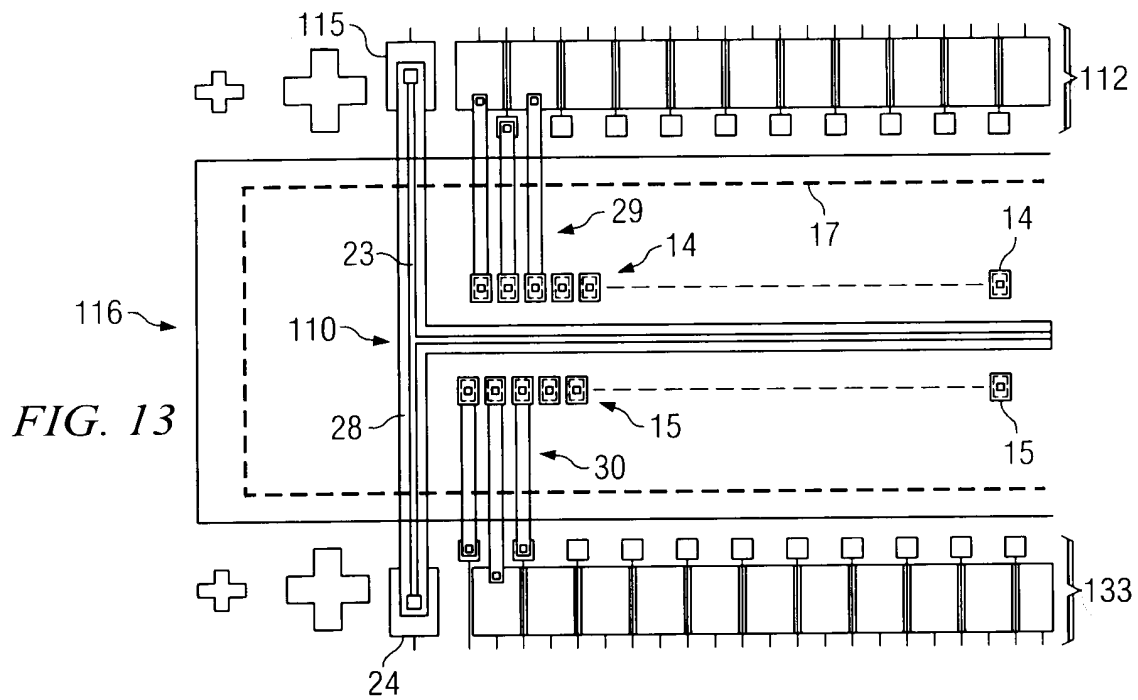
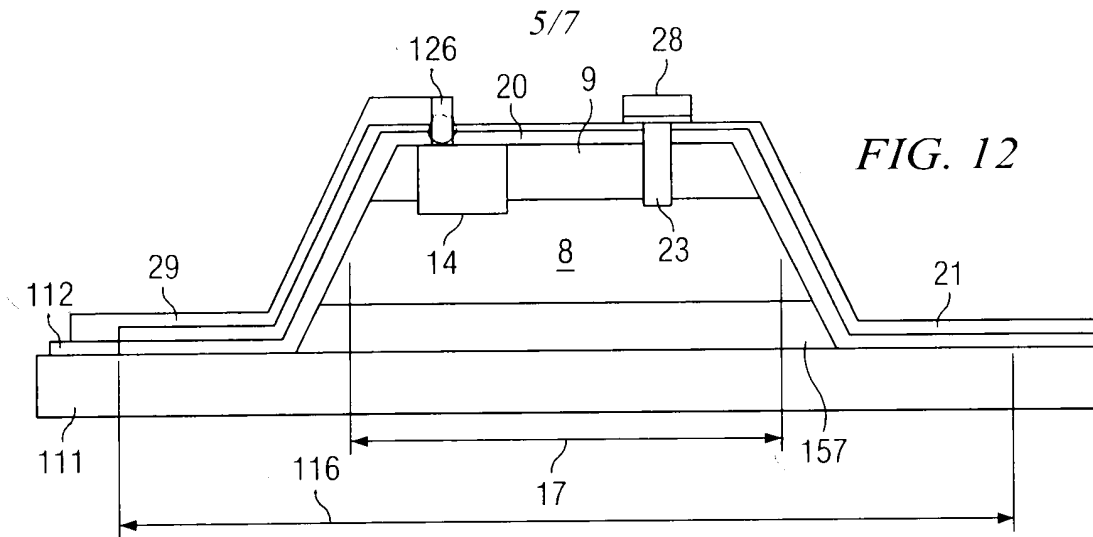


FIG. 9C





6/7

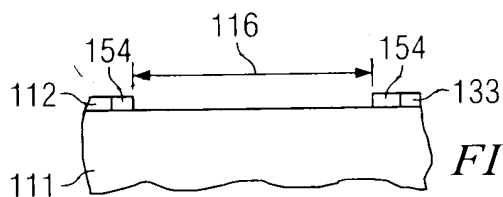


FIG. 15A

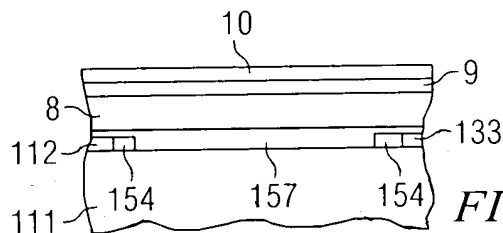


FIG. 15B

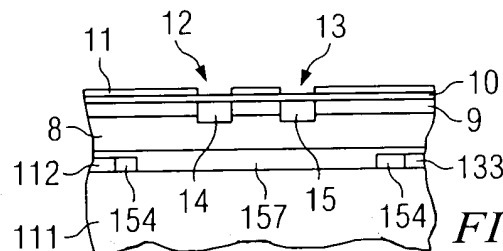


FIG. 15C

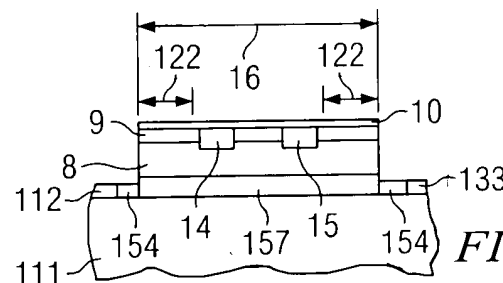


FIG. 15D

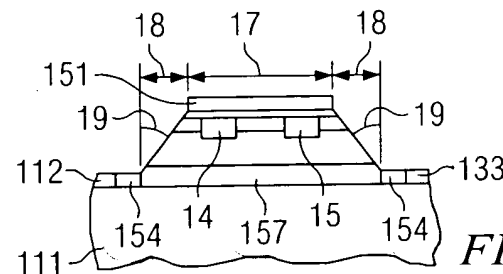


FIG. 15E

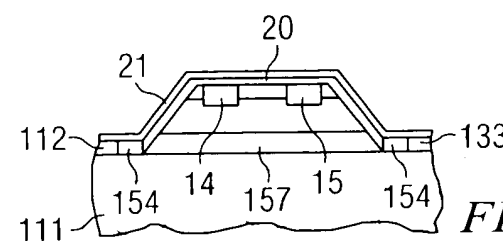


FIG. 15F

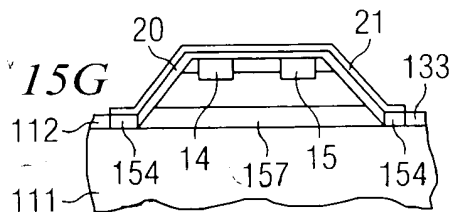


FIG. 15G

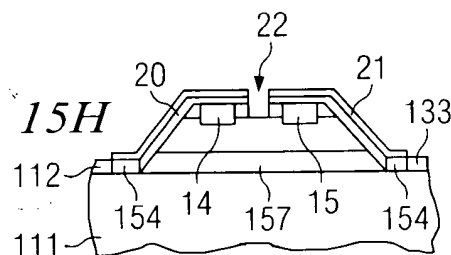


FIG. 15H

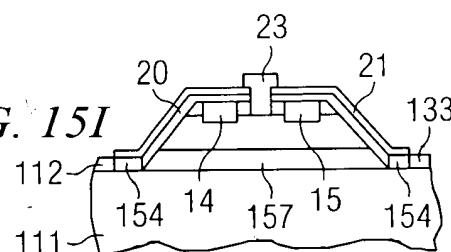


FIG. 15I

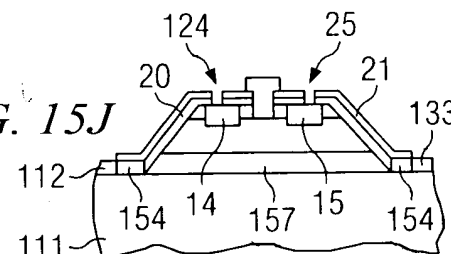


FIG. 15J

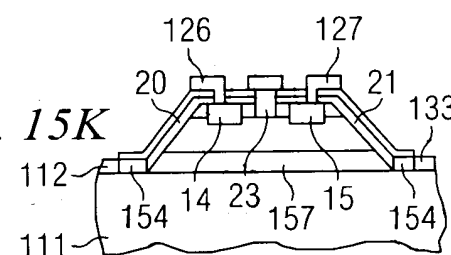


FIG. 15K

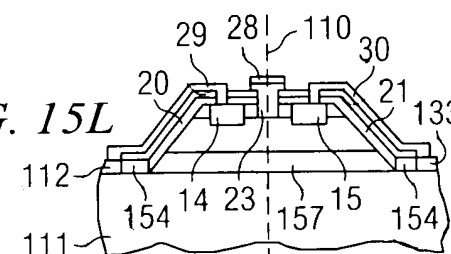


FIG. 15L

7/7

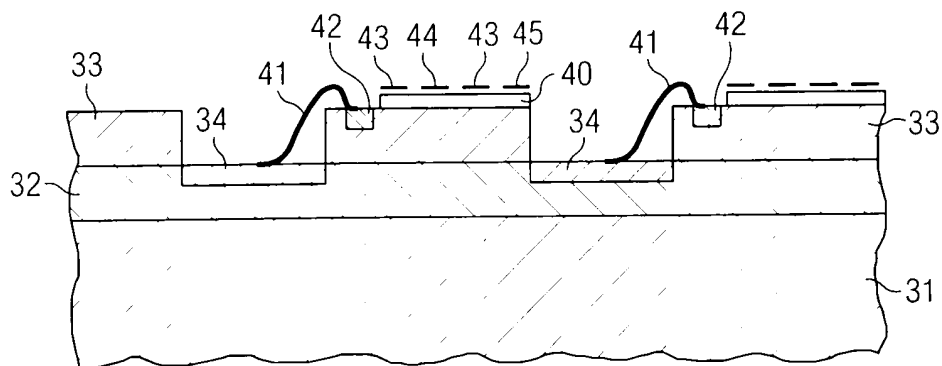


FIG. 16
 (PRIOR ART)

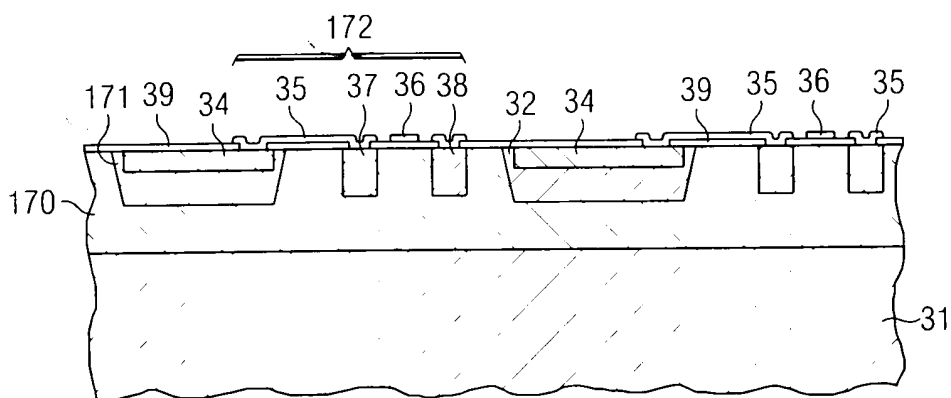


FIG. 17
 (PRIOR ART)

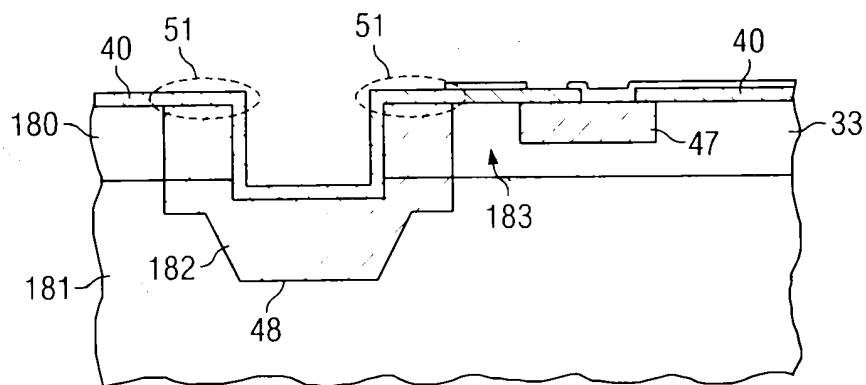


FIG. 18
 (PRIOR ART)